

HIGH-POWER SCALING FFAG RING STUDIES

D. J. Kelliher, S. Machida and G. H. Rees,
STFC Rutherford Laboratory, ASTeC, UK

Abstract

High-power FFAG rings are under study to serve as drivers for spallation neutrons, muon production, and accelerator-driven reactor systems. In this paper, which follows on from earlier work [1], a 20 - 70 MeV model for a high-power FFAG driver is described. This model would serve as a test bed to study topics such as space charge and injection in such rings. The design incorporates a long straight to facilitate H^- charge exchange injection. The dynamic aperture is calculated in order to optimize the working point in tune space. The injection scheme is also described. It is planned to experimentally study subjects relevant to high-power FFAGs using the KURRI FFAGs (ERIT and ADSR). Some simulation results of the ERIT FFAG ring are presented including the effects of space charge and foil scattering.

INTRODUCTION

In FFAG accelerators, the repetition rate is in principle limited only by the available rf voltage. Indeed the potential for FFAGs to accelerate high intensity beams was one of the motivations behind their revival in the 2000's in Japan [2],[3]. Space charge studies are planned, making use of the ERIT ring at KURRI, Japan. Some simulation results of ERIT are shown in the final section of this paper. In order to take the study of various aspects of intense proton beams to the next stage, building a dedicated FFAG may be required. This subject is discussed in the following sections.

FFAG MODEL

Taking a lead from KURRI, the study takes as its starting point a 100 Hz, 20 MeV, H^- linac injecting into a 20-70 MeV, FFAG, H^+ ring. An 8 cell DFD lattice is proposed with cell tunes $\nu_x = 0.401$, $\nu_y = 0.223$ and $\gamma_t = 2.3368$. The cell tunes are chosen to avoid principal resonances, but may be adjusted following a dynamic aperture survey. The F and D have opposite field directions, so a "return yoke free magnet" is proposed with magnetic shields to reduce end fields as used at KURRI. The edges of the magnet are radial. Each cell is mirror symmetric about the F centre with long drifts at either end.

The initial design work was carried out using a matrix code to model each momentum separately. In order to calculate the optics, the magnets are simulated as dipoles with quadrupole component and finite edge angles. The lattice parameters at injection and extraction used in the matrix code are listed in Table 1. In order to pursue further studies such as a calculation of dynamic aperture, the lattice was simulated by the Zgoubi tracking code.

Table 1: Lattice Parameters at Injection and Extraction

Parameter	Unit	Injection	Extraction
Short drift length	m	0.178	0.200
Long drift length	m	1.669	1.878
F length	m	1.450	1.632
D length	m	0.217	0.244
D bend angle	rad	-0.168	-0.168
F bend angle	rad	1.120	1.120
F, D norm. gradient	m^{-2}	± 0.541	± 0.685
Edge field extent	m	0.034	0.030
Mean radius	m	4.976	5.600

Table 2: Lattice Parameters in Zgoubi Model

Parameter	Unit	Value
Field index	-	4.345
Reference radius r_0	m	5.6
D&F Field at r_0	T	-1.078, 0.845
D&F radial extent	rad	0.044, 0.291
Edge field extent	m	0.034

In Zgoubi the magnets are simulated as radial FFAGs in which the reference radius r_0 , field B_0 , angular extent and field index k need to be specified. The field index is given by $k = g_n * r_m * \rho$ where g_n is the normalised gradient and r_m the mean radius at a particular momentum and ρ is the magnet bending radius. However there are a couple of significant differences between the matrix and Zgoubi models of the magnets.

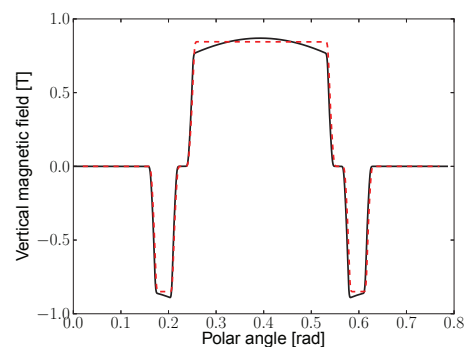


Figure 1: Comparison of vertical magnetic field along the closed orbit at the extraction momentum in one cell between the ASTeC matrix code STRING (black solid) and Zgoubi models (red dash).

In the matrix code the curvature of the lines of constant vertical field in the D is in the opposite sense to that in the F and, furthermore, the radius of curvature is equivalent to the bending radius. This ensures that the closed orbit at any momentum corresponds to a line of constant field (excepting the variation due to the end fields). By contrast in Zgoubi the curvature in the D is in the same sense as the F and the radius of curvature of the field lines is the machine radius. This results in a variation in the field and the gradient along the closed orbit and consequently different cell tunes than in the case of the matrix code. The difference in the field between the two codes is shown at the extraction momentum in Fig. 1.

By adjusting the field index and the D/F field ratio, the desired cell tunes in the tracking code are restored. Following this adjustment, the parameters used in the Zgoubi model are given in Table 2. As a further check of the degree of similarity between the two models from an optical point of view, the horizontal and vertical beta profiles calculated by the matrix and tracking codes are compared in Fig. 2.

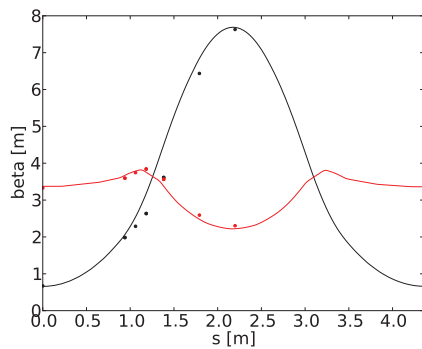


Figure 2: Comparison of beta profile calculated by Zgoubi (solid) with that calculated by the matrix code STRING (dots) in the horizontal (black) and vertical (red) planes.

DYNAMIC APERTURE

The dynamic aperture of the FFAG is calculated by means of single particle tracking. For each emittance tested, a single particle is chosen from the phase space ellipse. A small amplitude particle is tracked for 500 turns at the injection momentum. The amplitude is increased and the tracking repeated until the motion becomes unstable. The study began by checking the dynamic aperture in the horizontal plane with zero vertical amplitude ($y = y' = 0$) and assuming a lattice free of imperfections. In this case the aperture is 2500π mm mrad which is much greater than the 55π mm mrad needed for a 10^{13} proton bunch. The aperture appears to be limited by the sextupole-driven resonance at $\nu_x = 1/3$. The stable region within the dynamic aperture is shown in Fig. 3.

The calculation is then repeated but now including a vertical amplitude. Equal emittances are assumed in the horizontal and vertical plane at each stage. The dynamic aper-

ture is in this case significantly reduced to 200π mm mrad. Detuning with amplitude causes the vertical cell tune to approach $\nu_y = 0.25$ where it encounters a resonance driven by high order terms such as octupole. The vertical phase space is shown in Fig.4. The dynamic aperture is still more than required but may be reduced further when lattice imperfections and space charge effects are included.

As a first step towards establishing the optimal working point, the variation of dynamic aperture with vertical tune was calculated. The scan was limited to the interval $0.1875 < \nu_y < 0.25$ which, in this 8 cell lattice, is bounded by a half-integer and integer ring tune. The horizontal tune was kept fixed at nominal, $\nu_x = 0.4$. From the result of the scan, shown in Fig. 5, it is apparent that the general trend is for the dynamic aperture to decline as $\nu_y = 0.25$ is approached.

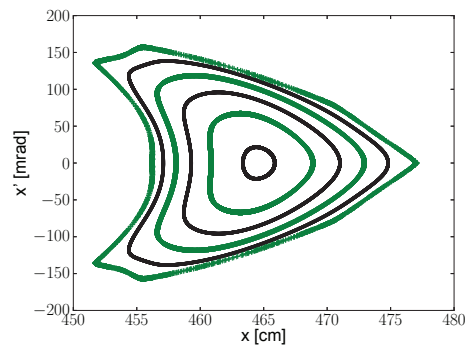


Figure 3: Stable region in horizontal phase space with a zero vertical emittance beam, no lattice imperfections and tracking for 500 turns. The innermost curve shows the required aperture.

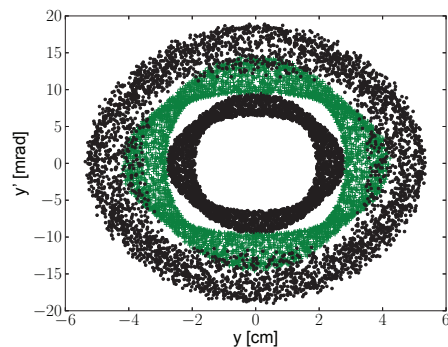


Figure 4: Stable region in vertical phase space with equal emittances in both planes, no lattice imperfections and tracking for 500 turns. The innermost curve shows the required aperture.

INJECTION

A multi-turn, H^- injection scheme is considered. The injection straight is too short to house a bump magnet chi-

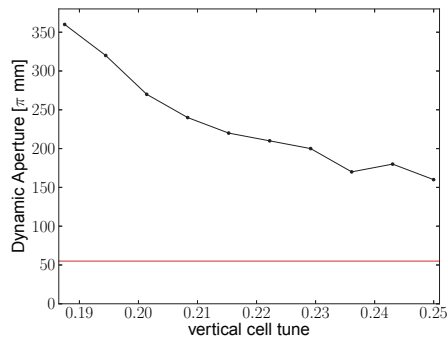


Figure 5: Dynamic aperture variation with vertical cell tune in the range $0.1875 < \nu_y < 0.25$ with horizontal cell tune fixed at $\nu_x = 0.4$. The red line show the required aperture.

cane, so the merging of incoming H^- ions and the recirculating protons has to occur in a lattice cell's bending-focusing region. Since the cells consist of DFD triplets, the proposed H^- stripping foil location is in a short drift between a D and F magnet within the end field region of the D magnet. The field level is chosen so stripped electrons bend to be collected outside the ring's acceptance.

Figure 6 is a schematic drawing of the proposed injection system. An injection septum magnet is not needed as H^- ions bend and focus in the opposite sense to protons. The input H^- beam ($\sim \pm 10\sigma$) is scraped to ($\sim \pm 5\sigma$) in the input line and directed to oscillate about or precisely follow the ring's closed orbit at the injection momentum. It is directed at a fixed spot on the foil, which is set on the vertical axis. Two steering magnets in the injection line sweep the beam vertically over a range of incident angles. In addition, the betatron phase space painting requires a programmed, collapsing horizontal orbit bump, together with a rf system frequency ramp. The beam centre at the foil is set at ($\sim \pm 5\sigma$) from the adjacent foil corner edges, so negative steering causes some input beam to miss the foil.

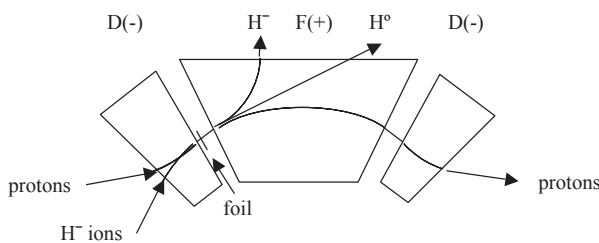


Figure 6: Schematic drawing for the multi-turn injection of H^- ions.

The horizontal injection orbit bump requires a pair of horizontal steering magnets on each side of the triplet set involved. Unstripped H^- ions and partially stripped H^0 atoms which remain after the foil, are collected on the outside of the FFAG ring, after passing through the following F magnet as indicated on Fig 6.

ISBN 978-3-95450-118-2

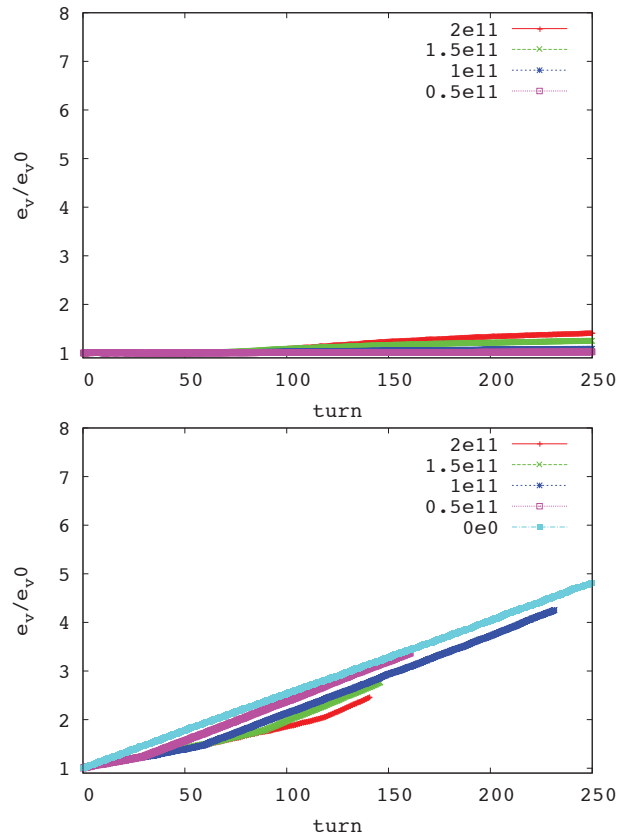


Figure 7: Emittance growth in ERIT in the vertical plane including the effect of just space charge (top) and both space charge and foil scattering (bottom) for a range of bunch intensities. The initial rms emittance is 8π mm mrad (unnormalised). The magnets are assumed to be perfectly aligned.

ERIT STUDIES

The ERIT FFAG at KURRI (Energy/Emittance Recovery Internal Target) is a 11 MeV proton storage ring designed to provide neutrons for BNCT (Boron Neutron Capture Therapy) located at the KURRI institute near Osaka, Japan. ERIT is made up of 8 FDF scaling triplet cells. Injection from a H^- linac is carried out using a carbon stripping foil. A Be foil internal target produces neutrons for use in BNCT. The energy lost through foil scattering is recovered with 18.1 MHz rf ($h = 6$). Important parameters for the ERIT ring are listed in Table 3.

Recently, an international collaboration has been initiated at KURRI to study subjects relevant to future high-power FFAGs, such as space charge and ionization cooling, making use of ERIT and the ADSR FFAGs. Space charge effects in FFAGs may differ from synchrotrons due to the intrinsic nonlinearities and the fact that, in general, the beam does not go through the centre of the beam pipe. Simulations of the ERIT and ADSR rings are ongoing before the commencement of experimental work.

The effects of both foil scattering and space charge in the ERIT ring was carried out using the SIMPSONS [4] code.

Table 3: Main ERIT Parameters

Parameter	Unit	Value
Field index	-	1.92
Mean radius r_0	m	2.35
F\D field ratio	-	3
Horizontal&Vertical tune	-	1.74, 2.22
Horizontal acceptance	mm mrad	7000π
Vertical acceptance	mm mrad	3000π
D&F Field at r_0	T	-0.727, 0.825

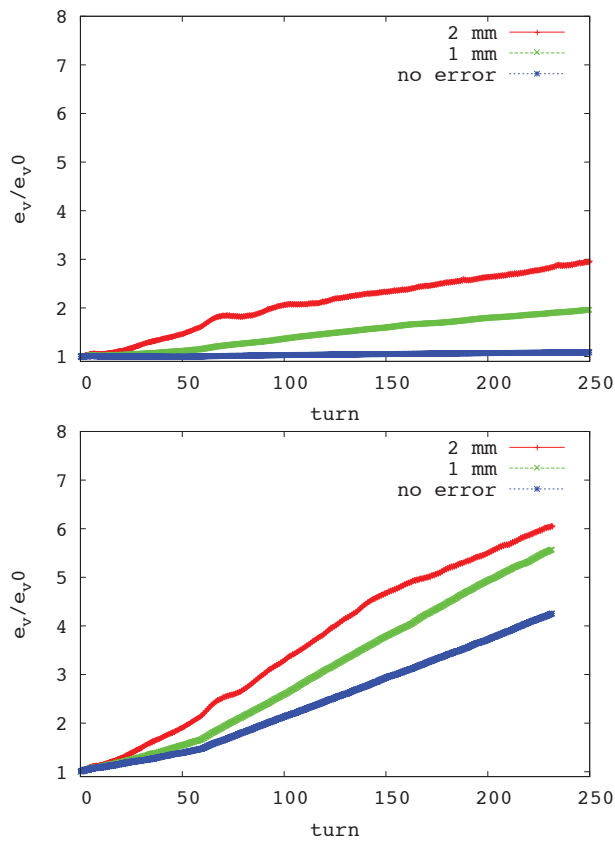


Figure 8: Emittance growth in ERIT in the vertical plane including the effect of just space charge (top) and both space charge and foil scattering (bottom) for a range of alignment errors. The intensity in all cases 1×10^{11} ppb.

It is estimated that the $20 \mu g cm^{-2}$ foil results in about 9 mean scattering events per proton per crossing, i.e. it falls in the plural scattering regime. However, the multiple-scattering Molière model is used in the simulation due to the availability of a look-up table and modest computational overhead. The foil scattering model in SIMPSONS is currently being upgraded - the results presented here are preliminary.

Figure 7 shows the relative contribution of space charge and foil scattering to emittance blow up calculated by SIMPSONS. It is clear that foil scattering is the dominant effect, possibly complicating plans to study space charge in ERIT. With the addition of alignment errors in the simula-

tion, the emittance growth is further increased as shown in Fig. 8 (note that due to the nonlinear field profile in FFAG magnets, misalignments introduce quadrupole as well as dipole errors).

DISCUSSION

Studies relevant to future high-power FFAG rings are ongoing. Simulations of the ERIT and ADSR rings will continue using SIMPSONS and other space charge codes. The preliminary results presented here indicate that the study of space charge in ERIT may be complicated by the effects of foil scattering. This is due to a lack of a bump magnet system in ERIT to move the injected beam away from the foil more rapidly. Future studies will inform experiments that will be carried out to investigate space charge in FFAGs.

REFERENCES

- [1] G.H. Rees and D.J. Kelliher, “A model for a high-power scaling FFAG ring design”, IPAC12, New Orleans, May 2012, MOPPD020, p. 409.
- [2] M. Aiba et al, “Development of FFAG proton synchrotron”, Proc. 7th European Particle Accelerator Conf., Vienna, Austria, 26-30 June 2000, p. 581.
- [3] Y. Mori, Nucl. Instr. Meth. Phys. Res. A562 (2006) 591.
- [4] S. Machida and M. Ikegami, AIP Conf. Proc. 448, 73 (1998).